

Induction of Stress Granule Assembly is Essential for the Orchestration of DNA Damage Response

Nicole S. Verkaik and Stephan P. Persengiev*

Department of Genetics, Erasmus MC,
Rotterdam 3000 CA, The Netherlands

*Corresponding author: Stephan Persengiev

e-mail: s.perseng@erasmusmc.nl

sperseng@yahoo.com

DNA damage provokes several responses including DNA repair, cell cycle regulation and apoptosis that collectively represent the DNA damage response (DDR). Here, we demonstrate that the DDR incorporates the activation of stress granule (SG) formation pathway as a mechanism to process destabilized RNAs. UV irradiation induced the assembly of SGs during the G2 phase and newly formed SGs appeared exclusively in the early G1 phase. SG assembly pathway was activated within the first hours after DNA damage, suggesting that the processing of destabilized RNAs is activated at an early stage. The induction of SGs and RNAi effector protein Argonaute 2 recruitment after UV exposure was independent of ATM and ATR signaling cascades. Apoptosis occurred only in SG-negative cells indicating that SGs promote cell survival after genotoxic stress. Analysis of several DNA damage/repair deficient MEFs revealed that the SG accumulation remained unaltered after UV exposure. Our results show that SGs are an essential component of DDR that is activated in parallel to the DNA damage kinase response networks.

Various endogenous and exogenous agents such as metabolic byproducts and natural UV irradiation continuously damage the cellular DNA. When not repaired properly, this can result in mutations or chromosomal aberrations and eventually trigger cancer. The mammalian cells have elaborate systems, collectively designated as DNA damage response (DDR) pathways, to counteract the harmful effects of DNA damage. Upon acute DNA damage, repair systems are activated in parallel with complex signal transduction routes that halt the cell cycle providing the cell with time to repair the damage or trigger apoptosis. Precise regulation of the DDR is critical for cell survival and its abrogation often results in genetic instability and malignant transformation, while the DDR hyper-activation may trigger excessive cell death and accelerate aging. Many DDR proteins are regulated at the post-translational level through modulation of protein activity or expression (Matsuoka et al. 2007). Additionally, the DDR is controlled at the transcriptional level by the induction of selected DNA repair and cell cycle regulatory genes after genotoxic stress (Garinis et al. 2005).

In response to genotoxic stress and other environmental stimuli mammalian cells undergo a selective translational arrest as an essential mechanism to preserve energy for the repair processes. Accumulation of protein components in the cytoplasm in the form of dynamically assembled structures referred to as processing bodies (PBs) and stress granules (SGs) is one of the hallmarks of translation abrogation (Anderson and Kedersha 2002; Anderson and Kedersha 2006). SGs are formed exclusively in response to stress encounters and appear to actively absorb aborted ribosomal/mRNA complexes to optimize further RNA processing. RNAi processing factor Argonaute 2 (Ago2) was found recently to be actively recruited to the SGs after translation inhibition in a miRNA-dependent manner (Leung et al. 2006; Calabrese et al. 2007; Leung and Sharp 2007). miRNAs mainly function as posttranscriptional repressors by binding to 3' untranslated regions of target messenger RNAs and are involved in diverse cellular and developmental processes in plants and animals including developmental timing, cellular asymmetry, cell growth, apoptosis and hematopoiesis (Brennecke et al. 2003; Cook et al. 2004; Grishok et al. 2005; Wassenegger 2005; Klattenhoff et al. 2007). A number of miRNAs have been found to associate with chromosome amplification, deletion and translocation suggesting involvements of miRNAs in the tumorigenesis (Calin et al. 2005; Zhang et al. 2006) (Kloosterman and Plasterk 2006).

Here we demonstrate that miRNA-mediated gene silencing is an active component of the DDR, which acts as an intermediate response between the fast changes in protein modifications

and the relatively slow transcriptional reprogramming after DNA damage. Moreover, we show that the activation of RNA silencing is cell cycle-dependent and plays an essential role in the regulation of cell survival, which might be important for carcinogenesis.

Results

UV Irradiation Leads to Formation of Stress Granules

We explored the possible involvement of RNA silencing in the regulation of mRNA processing after DNA damage. Recently, miRNAs have been found to relocalize to dynamically assembled perinuclear structures in response to stress stimuli identified as stress granules (SGs) (Anderson and Kedersha 2002). We interrogated whether UV-induced DNA damage leads to activation of RNAi pathways and SG formation in HeLa cells and primary human fibroblasts. SGs were visualized by immunofluorescent staining with TIA1 antibody at various time points following UV exposure. The results showed that UV irradiation led to a rapid perinuclear accumulation of SGs in HeLa cells and human fibroblasts (Figure 1A; Supplementary Figure 1A), suggesting that this is a general DDR-related phenomenon. The emergence of SGs was dose and time dependent and became apparent within approximately 1 hour after UV exposure. The number of SGs increased until they reached their maximum 4 hours after UV irradiation and were reduced to almost basal levels after 24 hours (Figure 1A and B; Supplementary Figure 1B). Thus, the cellular response to genotoxic stress incorporates SG formation, which strongly suggests that miRNA-mediated gene silencing is involved in the DDR.

SGs accumulation is cell cycle-dependent

Interestingly, SGs were not detected in the S-phase of the cell cycle, as judged by the absence of SGs in cells that showed bright H2AX foci, which have been found to form after replication as a result of UV-induced DNA lesions (Marti et al. 2006) (Figure 1C). However, only ~15% of H2AX negative cells formed SGs in asynchronously growing cells, suggesting that SG assembly might be cell cycle-dependent. Importantly, we observed that close to 100% of SG-positive cells appeared in pairs, and therefore might represent cells that have passed through mitosis and entered the G1 phase in spite of persisting DNA damage. To gain an insight into this issue we analyzed the SGs assembly after UV exposure using the classic thymidine block and release strategy. HeLa cells were synchronized at the G1/S phase, released from the block and UV irradiated at different time points. SGs accumulation was monitored by TIA-1 antibody staining 4 h after UV treatment. The results shown in Figure 2A and B revealed that

very few cells accumulated SGs after UV exposure during the G1 and S phases, in contrast to the massive increase of TIA-1-positive SGs (approximately 40% SGs-positive) in cells subjected to UV during the G2 phase. These cells apparently passed through mitosis because cell cycle profiling showed that 46% of the cells are in the G1 phase at the time of fixation. Thus, SGs formation is triggered by UV irradiation during the G2 phase, but fully assembled SGs were present only in G1 phase following M-phase transition (**Figure 2C**).

DNA Damage Induces Ago2 Relocalization to Stress Granules

Cytoplasmic bodies, including SGs, have been reported to serve as a depository for mRNAs after cellular stress and the recruitment of miRNA-programmed Ago2 to SGs after arsenite treatment suggested that SGs are the sites where mRNA processing occurs after cellular stress (Sen and Blau 2005)(Chu and Rana 2006; Leung et al. 2006). We reasoned that SG formation after UV induced DNA damage might also be associated with Ago2 relocalization (Cande et al. 2004; Meister et al. 2005; Anderson and Kedersha 2006). Therefore, we tested whether Ago2 actually translocates to SGs after DNA damage. We transfected HeLa cells with a previously described GFP-Ago2 transgene (Leung et al. 2006) and monitored its localization. Untreated cells showed GFP-Ago2 localization mainly to the cytoplasm, with accumulation in several small foci (Figure 3A). The association of GFP-Ago2 with small cytoplasmic structures in asynchronously growing cells has been described and the protein formations have been identified as processing bodies (PBs) (Eulalio et al. 2007). The intracellular Ago2 pattern changed markedly after UV irradiation: Ago2 accumulated in several large, newly formed structures in the perinuclear region, while PBs remained unchanged in other cells (Figure 3A, lower panel). The newly formed structures were identified as SGs by TIA1 costaining and exhibited complete colocalization of GFP-Ago2 and TIA-1.

To assess whether SGs accumulation after DNA damage depended on miRNAs presence we analyzed SG formation after UV exposure of Dicer-null ES cells. Immunostaining experiments shown in Figure 3B demonstrated that the Dicer knockout did not prevent the formation of SGs after UV exposure. Similar results were obtained after Dicer depletion by siRNA in HeLa cells (Supplementary Figure 2). Therefore, SG accumulation at the perinuclear compartment was independent of miRNA processing. However, Ago2 translocation to SGs was abrogated in Dicer-negative ES cells (Figure 3C). These data are consistent with the previously published observations that Argonaute programming by miRNAs is essential for its recruitment to the SGs (Leung et al. 2006). The observation has important functional implications because it

suggests that SGs provide the structural environment for the mRNA processing after genotoxic stress and miRNA-driven RNA silencing is an important, but dispensable feature of this process.

Ago2 Translocation to SGs is an Autonomous Process

The ATM and ATR DNA-damage checkpoint kinases are quickly activated in response to DNA damage and their recruitment to the DNA lesions plays a pivotal role in inducing cell cycle arrest, triggering apoptosis and optimizing DNA repair (Matsuoka et al. 2007) (Shiloh 2003). To investigate whether ATM and/or ATR play a role in the activation of Ago2-SGs pathway, we treated GFP-Ago2 HeLa cells derivatives with either caffeine in a concentration that inhibits both ATR and ATM or the ATM inhibitor KU55933 before UV irradiation (Jazayeri et al. 2006). As expected, caffeine blocked UV-induced ATR activity (Supplementary Figure 3) and KU55933 inhibited ATM activation upon ionizing radiation (data not shown). Surprisingly, inhibition of ATM and ATR had no apparent effect on SGs formation and Ago2 accumulation after UV-induced exposure (Figure 3D and E). The number of SG-positive cells and colocalization with Ago2 remained unaltered, indicating that ATM and ATR controlled checkpoints were not required for the Ago2 translocation to SGs assembly.

Several reports have implicated the p38/MAPK pathway in DNA damage response networks and established its independence of the ATM/ATR signaling cascades (Boutros et al. 2006; Rodriguez-Bravo et al. 2006; Reinhardt et al. 2007). We therefore tested whether the inhibition of MAPKAP Kinase-2 (MK2), a critical downstream target of p38/MAPK (Reinhardt et al. 2007), might affect the accumulation of SGs. HeLa cells were treated with a low dose of UCN-01, an MK2 and Chk1 inhibitor that dramatically increase UV sensitivity (Reinhardt et al. 2007). However, SGs accumulation after UV exposure was not affected by UCN-01, indicating that p38/MAPK signaling was not essential for the SGs formation (Figure 3E and Supplementary Figure 3). We also tested whether the SG accumulation is affected in MEFs rendered deficient for several key DNA repair and damage response genes including p53 and Nbs1 DNA damage response genes. A summary of these experiments presented in Table 1 revealed that SG aggregation remained intact after UV exposure despite the targeted disruption of key DNA damage response networks. Thus, the assembly of SGs is an autonomous process that functions in parallel with the classical DNA damage response pathways.

miRNAs processing inhibition and SGs breakdown promotes apoptosis

Next, we investigated the possible functional consequences of miRNA-directed gene silencing in the DDR. We first asked whether the transient SGs accumulation after UV exposure was associated with apoptosis induction. HeLa cells were UV irradiated and apoptotic cells were identified by immunostaining with antibodies against cleaved caspase-3. Cleaved caspase-3 staining was detected in more than 50% of the cells at 24 hours after UV irradiation, while TIA1 positive SGs persisted in approximately 1% of the cells. Surprisingly, no SGs were observed in more than 10^4 cleaved caspase3-positive cells (Figure 5A and B). Thus, SGs presence was incompatible with cell death induction and suggested that SGs breakdown might be an indicator and/or a prerequisite for irreversible apoptosis activation.

Finally, we addressed the role of miRNAs processing in cell survival after UV irradiation. Ago2 and Dicer were knocked down and the cell proliferation rate was determined by counting the relative number of viable cells at 0, 24, 48 and 72 hours after UV irradiation. Ago2 and Dicer depletion caused a growth delay in the first 24 hours after cell plating, but all cells had a similar cell proliferation rate at later time points (Supplementary Figures 4 and 8). We observed a significant reduction in cell survival of Ago2 and Dicer siRNA treated cells at 48 and 72 hours after UV exposure, demonstrating that miRNA mediated gene silencing is important for cell survival after DNA damage (Figure 5C).

Discussion

In this report through a combination of fluorescence microscopy, genome-wide miRNA profiling and reverse genetics we describe a novel role for the miRNA-driven RNA silencing machinery in the DNA damage response. Based upon the observations that the SGs assembly after UV exposure depended on the miRNAs presence and the failure to assemble SGs in cells undergoing apoptosis, we conclude that the SGs formation is most likely an indicator for a selective time-coordinated mRNA repression and delayed apoptosis activation.

Following DNA damage a number of factors translocate to the damaged sites to facilitate the repair process and induce cell cycle arrest. The DNA repair centers consists of large number of proteins, but ATM and ATR phosphatidylinositol 3-kinase-like kinases are primarily responsible for the coordination of cellular responses to genotoxic stress(Lee and Paull 2005). In addition, p38MAPK/MK2 pathway was found to play a major in cell cycle arrest and survival after DNA damage (Reinhardt et al. 2007). The autonomy of Ago2 translocation and SGs

accumulation from ATM, ATR and p38/MAPK response pathways was unexpected. These results argue that miRNA-driven RNA silencing pathway functions in parallel with the ATM/ATR signaling cascades and eventually has the potential to limit their activity, as recently suggested for the rasiRNAs (Klattenhoff et al. 2007).

Ago2 was found to interact with several protein complexes associated with the SGs and PBs (Meister et al. 2005; Chu and Rana 2006). However, the association of Argonaute protein with PBs did not require miRNAs suggesting that the ribosome-free PBs are not likely to be the sites where miRNA-directed RNA repression occurs (Leung et al. 2006). The loading of Ago2 with miRNAs appears to be the initial trigger for the SGs formation. However, the induction of miRNA expression after UV irradiation is unlikely to be solely accountable for this phenomenon. Only cells irradiated during the G2 phase acquire SGs following passage through mitosis indicating that additional cell cycle associated factors are essential for SGs assembly. Moreover, the data suggest that miRNA mediated gene silencing can be accomplished without relocalization of RISC complexes in cells irradiated during the G1 and S phases. However, the observation that SG formation is initiated during the G2 phase following UV exposure has important implications. Cells are not able to undergo apoptosis during the G2 phase and inability to enforce the G2 checkpoint immediately after DNA damage might lead to mitotic catastrophe and genomic aberrations. Therefore, the activation of SGs assembly pathway after UV exposure might serve to ensure cell passage through mitosis and G1 entry, when the apoptosis machinery can be activated if necessary. The mechanism of SGs accumulation during G1 phase after DNA damage is not entirely clear but the inability to coordinate transcription activation during M/G1 transition phase, as well as the release of damaged nuclear components (e.g. damaged or truncated RNAs) into the cytoplasm might be contributing factors.

Our results taken into the context of the current information on SGs protein organization suggest that SGs main DDR function is to provide a platform for the recruitment of RNA modifying enzymes involved in the processing of destabilized RNAs. Moreover, the time-restricted activation of the RNA silencing pathways after DNA damage suggest that the DNA damage response is temporally organized and might be divided into a fast, intermediate and slow component (Figure 6). Initial rapid response leading to protein modifications and proteosomal degradation is necessary to react to the genotoxic stress and prevent direct adverse effects. Subsequently, the miRNA-mediated translational repression is activated to prevent *de novo* protein synthesis, which might otherwise initiate a futile cycle of protein

synthesis and degradation. Finally, transcriptional reprogramming takes over the control of the cellular response to DNA damage in order to stabilize the gene expression.

Integration of the DNA damage response with cellular metabolism determines the cell fate after genotoxic insult. At the organismal level, if DDR it is not adequately controlled, the result might be either premature aging caused by the loss of stem cells or inability to initiate apoptosis, which may lead to malignant transformation. Therefore, the miRNA-stress granules response might be crucial for the cell fate determination after genotoxic insults. Maintenance of cell viability for several hours after DNA damage until cell cycle checkpoints are fully activated may provide the necessary time window for the cell either to repair or trigger a coordinated apoptotic response.

Experimental Procedures

Cell Culture and Genotoxic Stress Induction

HeLa cells and human fibroblasts were grown in Dulbecco's modified Eagle's medium (DMEM; Gibco-BRL) supplemented with 10% heat-inactivated fetal calf serum (FCS). *Dicer*^{-/-} ES cells were grown on gelatin-coated plates with media supplemented with leukemia inhibitory factor (Murchison et al. 2005). For induction of stress, cells were washed twice with phosphate buffered saline (PBS) without Mg²⁺ and Ca²⁺, pH 7.5. Genotoxic stress was induced when cells were 50%–70% confluent by 8, 10 or 20 J/m² UVC irradiation. Where indicated HeLa cells or human fibroblasts were treated with the specific ATM kinase inhibitor KU55933 (10 μM) (Kudos Pharmaceuticals, UK), caffeine (ATM/ATR inhibitor, 8 mM) (Sigma) and Chk1 inhibitor UCN-01 (300 nM). UCN-01 was obtained from the Drug Synthesis and Chemistry Branch, NIH (Bethesda, MD).

Cell synchronization and cell cycle profiling

Cells were arrested at the G1/S boundary by incubation in medium containing 4 mM thymidine for 24 h. Cells were released from the thymidine for 18 h before a second incubation 4 mM thymidine for 24 h. Cells were released from the thymidine, subjected to 20 J/m² UV irradiation at different time points and cell cycle profiling by PI exclusion and indirect immunofluorescence analysis were carried out at 0, 4, 8 and 24 h.

Immunofluorescence analysis

For immunofluorescence analysis, cells were fixed either with 2% paraformaldehyde or methanol for 15 min at room temperature or 20 min at 20 C. and permeabilized and blocked with PBS containing 5% BSA and 0.1% Triton X-100 for 30 min. The anti-TIA-1 (Santa Cruz Biotech) and activated caspase 3 (Cell Signaling) antisera were used at 1:100 dilution and H2AX (Upstate Biotech) antibody at 1:500 dilution. Secondary anti-goat and anti-rabbit antibodies labeled with Alexa 488 and Alexa 594 fluorochromes, respectively (Molecular Probes) were used at 1:1000 dilutions.

Cell transfections and siRNA experiments

GFP-Ago2 transfections of HeLa and Dicer-null ES cells were performed using Fugene transfection reagent (Roche). Knockdown experiments were performed in HeLa cells by employing Dicer and Ago2 specific siRNAs (Sigma) at 50 nM final concentrations (see Table S1 for siRNA primer sequences). All transfections were performed using Oligofectamine (Life Technologies) for 48 h or 72 h, as recommended by the manufacturer. The siRNA

RNA and protein analysis

Total RNA prepared from cultured cell lines and tissue samples by Trizol (Invitrogen). GAPDH, Dicer and Ago2 levels were monitored by RT-PCR. The gene-specific primers for GAPDH, Ago2 and Dicer are shown in Table S1. Immunoblot assays were performed using polyclonal antibodies that specifically recognized Ago2 (Upstate), anti-phospho Chk1S317 (Bethyl Laboratories, Inc.) and GRB2 and Dicer (Abcam).

Cell viability assay

HeLa cells were treated with Dicer and Ago2 siRNAs (50 nM) for 72 h. Cells were subjected to UV irradiation (10 J/m²), transfected again with Dicer and Ago2 siRNAs and cell viability was

determined by Trypan blue exclusion at different times points. The effectiveness of Dicer and Ago2 knockdowns was determined by RT-PCR and western blotting.

References

- Anderson, P. and N. Kedersha. 2002. Stressful initiations. *J Cell Sci* **115**: 3227-34.
- . 2006. RNA granules. *J Cell Biol* **172**: 803-8.
- Boutros, R., C. Dozier, and B. Ducommun. 2006. The when and wheres of CDC25 phosphatases. *Curr Opin Cell Biol* **18**: 185-91.
- Brennecke, J., D.R. Hipfner, A. Stark, R.B. Russell, and S.M. Cohen. 2003. bantam encodes a developmentally regulated microRNA that controls cell proliferation and regulates the proapoptotic gene hid in Drosophila. *Cell* **113**: 25-36.
- Calabrese, J.M., A.C. Seila, G.W. Yeo, and P.A. Sharp. 2007. RNA sequence analysis defines Dicer's role in mouse embryonic stem cells. *Proc Natl Acad Sci U S A* **104**: 18097-102.
- Calin, G.A., M. Ferracin, A. Cimmino, G. Di Leva, M. Shimizu, S.E. Wojcik, M.V. Iorio, R. Visone, N.I. Sever, M. Fabbri, R. Iuliano, T. Palumbo, F. Pichiorri, C. Roldo, R. Garzon, C. Sevignani, L. Rassenti, H. Alder, S. Volinia, C.G. Liu, T.J. Kipps, M. Negrini, and C.M. Croce. 2005. A MicroRNA signature associated with prognosis and progression in chronic lymphocytic leukemia. *N Engl J Med* **353**: 1793-801.
- Cande, C., N. Vahsen, D. Metivier, H. Tourriere, K. Chebli, C. Garrido, J. Tazi, and G. Kroemer. 2004. Regulation of cytoplasmic stress granules by apoptosis-inducing factor. *J Cell Sci* **117**: 4461-8.
- Chu, C.Y. and T.M. Rana. 2006. Translation repression in human cells by microRNA-induced gene silencing requires RCK/p54. *PLoS Biol* **4**: e210.
- Cook, H.A., B.S. Koppetsch, J. Wu, and W.E. Theurkauf. 2004. The Drosophila SDE3 homolog armitage is required for oskar mRNA silencing and embryonic axis specification. *Cell* **116**: 817-29.
- Eulalio, A., I. Behm-Ansmant, and E. Izaurralde. 2007. P bodies: at the crossroads of post-transcriptional pathways. *Nat Rev Mol Cell Biol* **8**: 9-22.
- Garinis, G.A., J.R. Mitchell, M.J. Moorhouse, K. Hanada, H. de Waard, D. Vandeputte, J. Jans, K. Brand, M. Smid, P.J. van der Spek, J.H. Hoeijmakers, R. Kanaar, and G.T. van der Horst. 2005. Transcriptome analysis reveals cyclobutane pyrimidine dimers as a major source of UV-induced DNA breaks. *Embo J* **24**: 3952-62.

- Grishok, A., J.L. Sinskey, and P.A. Sharp. 2005. Transcriptional silencing of a transgene by RNAi in the soma of *C. elegans*. *Genes Dev* **19**: 683-96.
- Jazayeri, A., J. Falck, C. Lukas, J. Bartek, G.C. Smith, J. Lukas, and S.P. Jackson. 2006. ATM- and cell cycle-dependent regulation of ATR in response to DNA double-strand breaks. *Nat Cell Biol* **8**: 37-45.
- Klattenhoff, C., D.P. Bratu, N. McGinnis-Schultz, B.S. Koppetsch, H.A. Cook, and W.E. Theurkauf. 2007. *Drosophila* rasiRNA pathway mutations disrupt embryonic axis specification through activation of an ATR/Chk2 DNA damage response. *Dev Cell* **12**: 45-55.
- Kloosterman, W.P. and R.H. Plasterk. 2006. The diverse functions of microRNAs in animal development and disease. *Dev Cell* **11**: 441-50.
- Lee, J.H. and T.T. Paull. 2005. ATM activation by DNA double-strand breaks through the Mre11-Rad50-Nbs1 complex. *Science* **308**: 551-4.
- Leung, A.K., J.M. Calabrese, and P.A. Sharp. 2006. Quantitative analysis of Argonaute protein reveals microRNA-dependent localization to stress granules. *Proc Natl Acad Sci U S A* **103**: 18125-30.
- Leung, A.K. and P.A. Sharp. 2007. microRNAs: A Safeguard against Turmoil? *Cell* **130**: 581-5.
- Marti, T.M., E. Hefner, L. Feeney, V. Natale, and J.E. Cleaver. 2006. H2AX phosphorylation within the G1 phase after UV irradiation depends on nucleotide excision repair and not DNA double-strand breaks. *Proc Natl Acad Sci U S A* **103**: 9891-6.
- Matsuoka, S., B.A. Ballif, A. Smogorzewska, E.R. McDonald, 3rd, K.E. Hurov, J. Luo, C.E. Bakalarski, Z. Zhao, N. Solimini, Y. Lerenthal, Y. Shiloh, S.P. Gygi, and S.J. Elledge. 2007. ATM and ATR substrate analysis reveals extensive protein networks responsive to DNA damage. *Science* **316**: 1160-6.
- Meister, G., M. Landthaler, L. Peters, P.Y. Chen, H. Urlaub, R. Luhrmann, and T. Tuschl. 2005. Identification of novel argonaute-associated proteins. *Curr Biol* **15**: 2149-55.
- Murchison, E.P., J.F. Partridge, O.H. Tam, S. Cheloufi, and G.J. Hannon. 2005. Characterization of Dicer-deficient murine embryonic stem cells. *Proc Natl Acad Sci U S A* **102**: 12135-40.

- Reinhardt, H.C., A.S. Aslanian, J.A. Lees, and M.B. Yaffe. 2007. p53-deficient cells rely on ATM- and ATR-mediated checkpoint signaling through the p38MAPK/MK2 pathway for survival after DNA damage. *Cancer Cell* **11**: 175-89.
- Rodriguez-Bravo, V., S. Guaita-Esteruelas, R. Florensa, O. Bachs, and N. Agell. 2006. Chk1- and Claspin-Dependent but ATR/ATM- and Rad17-Independent DNA Replication Checkpoint Response in HeLa Cells. *Cancer Res* **66**: 8672-8679.
- Sen, G.L. and H.M. Blau. 2005. Argonaute 2/RISC resides in sites of mammalian mRNA decay known as cytoplasmic bodies. *Nat Cell Biol* **7**: 633-6.
- Shiloh, Y. 2003. ATM and related protein kinases: safeguarding genome integrity. *Nat Rev Cancer* **3**: 155-68.
- Wassenegger, M. 2005. The role of the RNAi machinery in heterochromatin formation. *Cell* **122**: 13-6.
- Zhang, L., J. Huang, N. Yang, J. Greshock, M.S. Megraw, A. Giannakakis, S. Liang, T.L. Naylor, A. Barchetti, M.R. Ward, G. Yao, A. Medina, A. O'Brien-Jenkins, D. Katsaros, A. Hatzigeorgiou, P.A. Gimotty, B.L. Weber, and G. Coukos. 2006. microRNAs exhibit high frequency genomic alterations in human cancer. *Proc Natl Acad Sci U S A* **103**: 9136-41.

Acknowledgments

This work does not represent the official line of research of the Genetics Department at ErasmusMC. The experiments presented in this study were conceived by Stephan Persengiev and he wrote the manuscript. Nicole Verkaik performed the immunostaining experiments. We thank Philip Sharp and Anthony Leung for providing the GFP-Ago2 expression vector and Van Ta for analyzing FACS data. The authors are indebted to Gregory Hannon and Elizabeth Murchison for providing the Dicer-deficient ES cells.

Figure 1

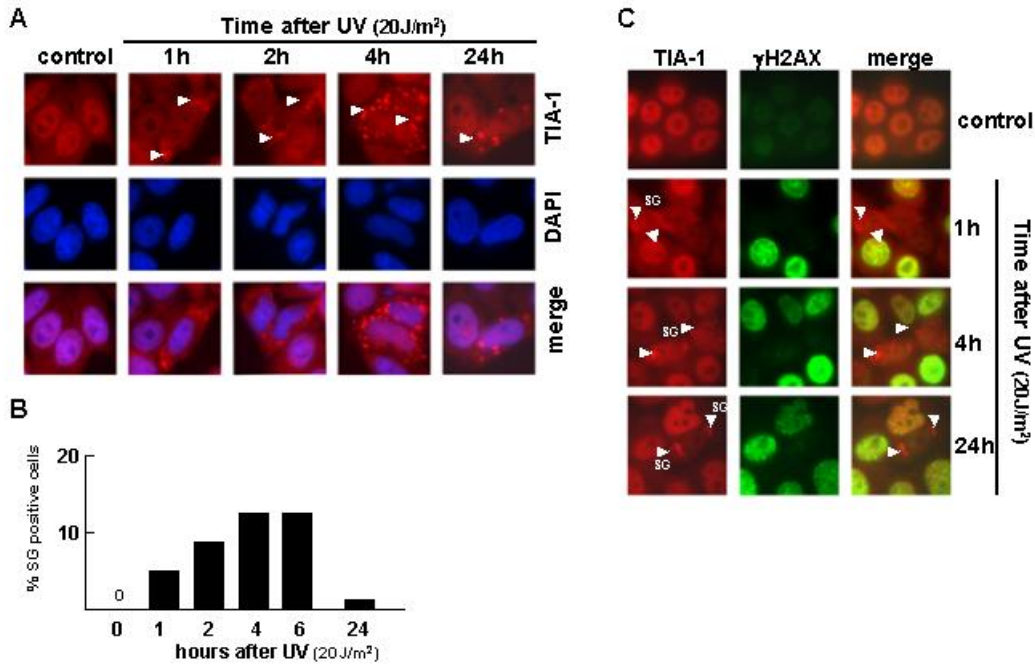


Figure 1. SG formation after UV irradiation.

A. Time-course analysis of TIA-1 accumulation after UV irradiation. HeLa cells were subjected to 20 J/m² UV and accumulation of SGs was monitored by staining for TIA1.

B. Quantification of cells containing stress granules (SGs) after UV irradiation. For unirradiated cells >10⁴ cells have been counted. For irradiated cell cultures an average of 500 cells have been counted and SG-positive cells are presented as a percentage of total population.

C. SG formation is not present in S-phase cells. Immunofluorescence imaging of H2AX and TIA-1 in HeLa cells following irradiation with 20 J/m² UV. H2AX foci at damaged sites are formed during the S-phase when UV induced DNA lesions are converted into double strand breaks.

Figure 2

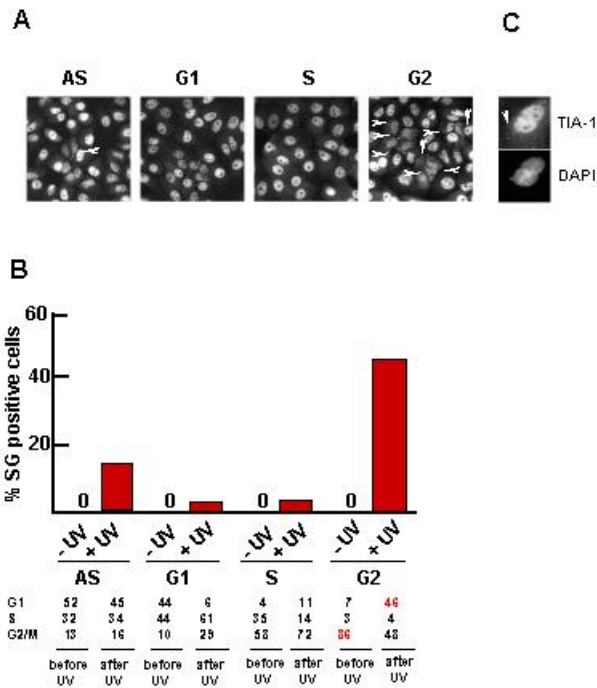


Figure 2. SGs accumulation is cell cycle restricted.

A. SGs accumulation after release from double thymidine block. Cells were UV irradiated at 0, 4 and 8 hours after release from thymidine block and stained with TIA-1 antibody 4 h later. Cell cycle profiling was carried out before and 4 h after UV exposure at each time point. Cells were irradiated in G1, S and G2 cell cycle phases. AS – asynchronous cells. SGs are indicated by arrows.

B. Quantification of SG-positive cells subjected to UV irradiation during different cell cycle stages. Cell cycle profiles before and after irradiation are shown.

C. A higher magnification image reveals that SGs are formed at a very early G1 phase immediately after the telophase/cytokinesis stage following UV exposure in G2. Arrow indicates newly formed SGs.

Figure 3

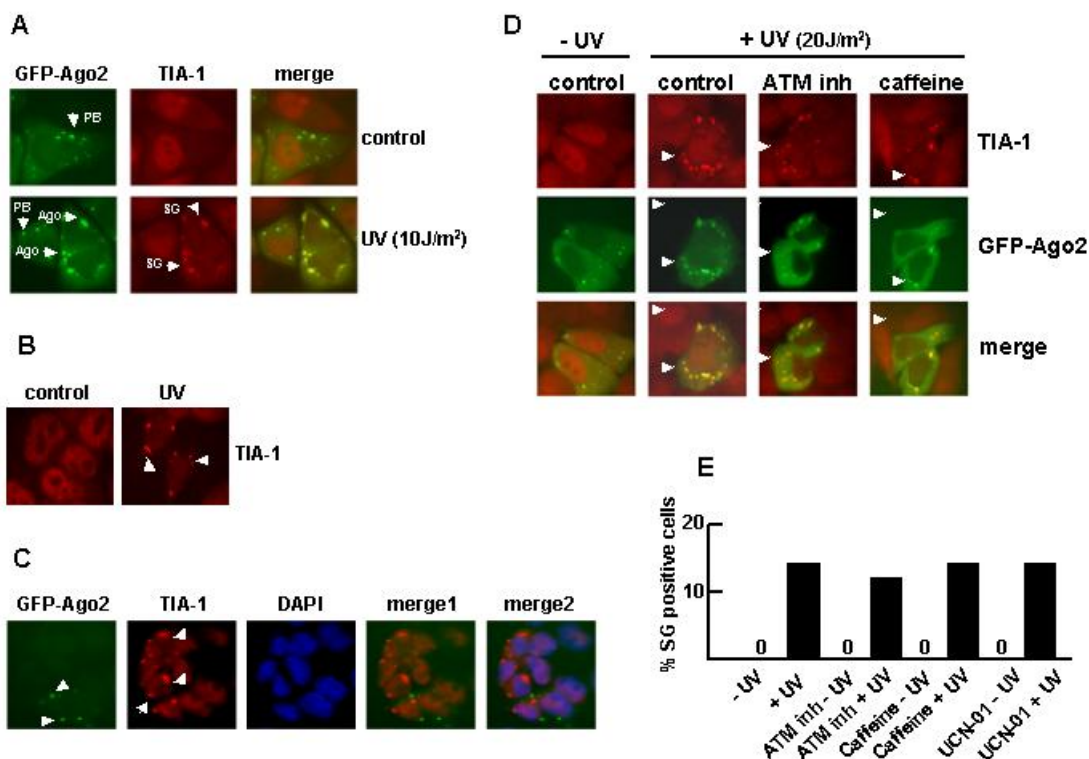


Figure 3. SG formation is independent of DNA damage signal cascades and miRNA processing.

A. Ago2 translocates to SGs after DNA damage. HeLa cells were transfected with a GFP-Ago2 transgene and Ago2 translocation to SGs at 4 hours after UV irradiation (10 J/m²) was confirmed by costaining for TIA-1.

B. SGs accumulate in the absence of miRNAs. Dicer-null ES cells were subjected to UV and SGs formation was monitored by staining with a TIA-1 antiserum.

C. Ago2 translocation to SGs is abrogated in Dicer-null ES cells. ES cells were transfected with a GFP-Ago2 transgene and Ago2 subcellular localization and SG accumulation 4 hours after UV irradiation (20 J/m²) were visualized. The arrows indicate the localization of Ago2 and SGs after UV exposure.

D. GFP-Ago2 translocation to SGs after genotoxic stress is independent of ATM and ATR kinase activities and p38/MAPK signaling. HeLa cells were treated with either the ATM inhibitor KU55933 or caffeine and Ago2 relocalization to SGs was monitored 4 hours after UV irradiation (20 J/m²). Arrows indicate SGs and GFP-Ago2 localization.

E. Quantification SG positive HeLa cells 4 hours after UV irradiation (20 J/m²) in combination with the ATM inhibitor KU55933, caffeine or the Chk1/MK2 inhibitor UCN-01. An average 500

cells have been counted for UV-treated cells and $>10^4$ cells for non-irradiated cells. SG-positive cells are presented as a percentage of total population.

| genotype | (-) UV | (+) UV | DNA response/repair defect |
|-----------------------|--------|--------|----------------------------|
| WT MEFs | No | Yes | |
| XPA ^{-/-} | No | Yes | Nucleotide excision repair |
| Ku70 ^{-/-} | No | Yes | NHEJ/DNA damage signaling |
| Ku80 ^{-/-} | No | Yes | NHEJ |
| NBS1 ^{-/-} | No | Yes | DNA damage signaling |
| Rad54 ^{-/-} | No | Yes | Homologous recombination |
| DNA-PK ^{-/-} | No | Yes | NHEJ/DNA damage signaling |
| p53 ^{-/-} | No | Yes | Checkpoint/apoptosis |
| Dicer ^{-/-} | No | Yes | MIRNA deficient ES cells |

Table 1. Summary of SG presence before and after UV irradiation in MEFs with targeted mutations for various DNA damage response genes.

Figure 4

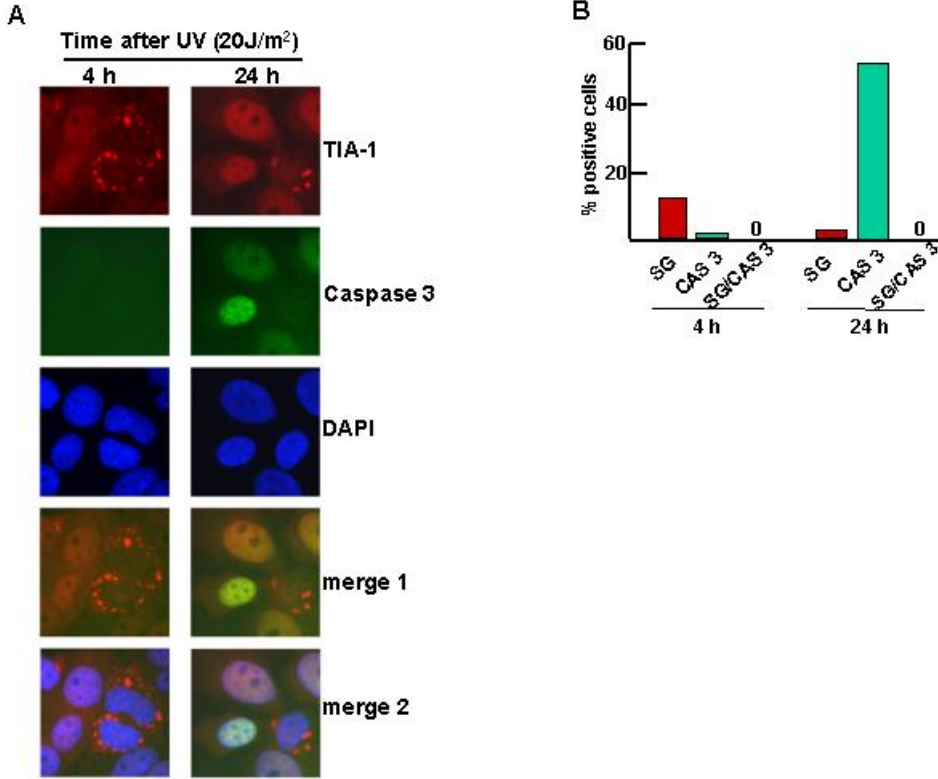


Figure 4. miRNA mediated gene silencing is important for cell survival after UV treatment.

A. Activation of the apoptotic response is mutually exclusive with SGs. HeLa cells were subjected to 20 J/m² UV and accumulation of TIA-1 labeled SGs and caspase-3 was monitored by indirect immunofluorescence.

B. Quantification of SG-positive, cleaved caspase-3 (CAS3)-positive and SG/CAS3-positive cells 4h and 24 h after UV exposure.

C. Cell survival after UV treatment is reduced in HeLa cells treated with Ago2 or Dicer siRNAs. Cells were treated either with a control siRNA, Dicer or Ago2 siRNAs for 72 hours. Then viable cells were re-plated and exposed to UV (10 J/m²) or mock-treated. The number of viable cells was counted at 0, 24, 48 and 72 hours after UV exposure. The relative number of viable cells after UV irradiation is shown as fraction of the viable cells after mock-treatment.

Supplementary Figures

Figure S1

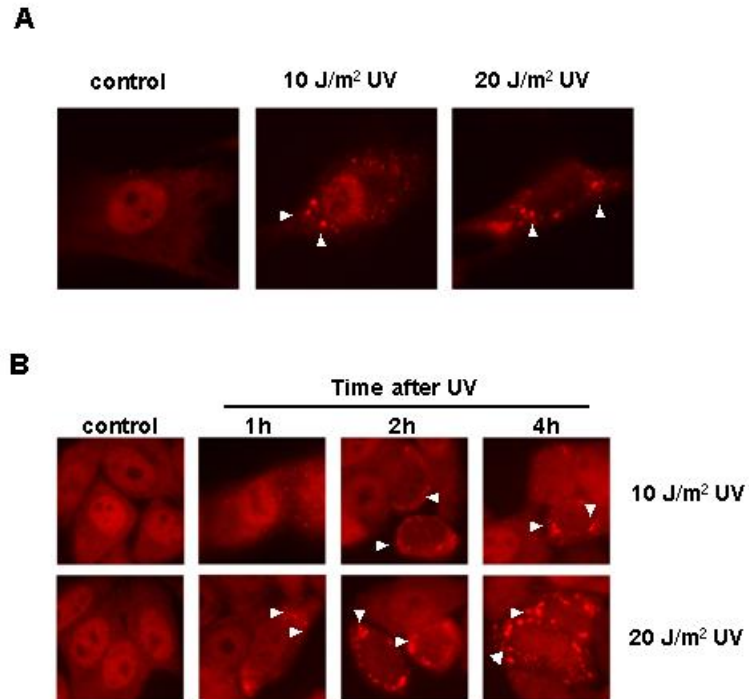


Figure S1. TIA-1 staining of SGs after 10 and 20 J/m² UV irradiation.

A. Human primary fibroblasts were subjected to 10 or 20 J/m² UV irradiation and indirect immunofluorescence analysis was carried out with a TIA-1 antibody that specifically recognized SGs.

B. HeLa cells were subjected to 10 or 20 J/m² UV irradiation and indirect immunofluorescence analysis was carried out with a TIA-1 antibody.

Figure S2

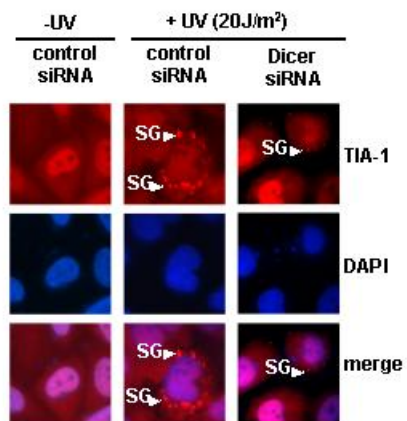


Figure S2. SG fomation is independent of miRNA processing enzyme Dicer

HeLa cells were transfected with either a non-specific (NS) or Dicer specific siRNA for 72 hours. SGs was monitored 4 hours after UV treatment (20 J/m²) by staining with a TIA-1 antibody. Arrows indicate SGs localization.

Figure S3

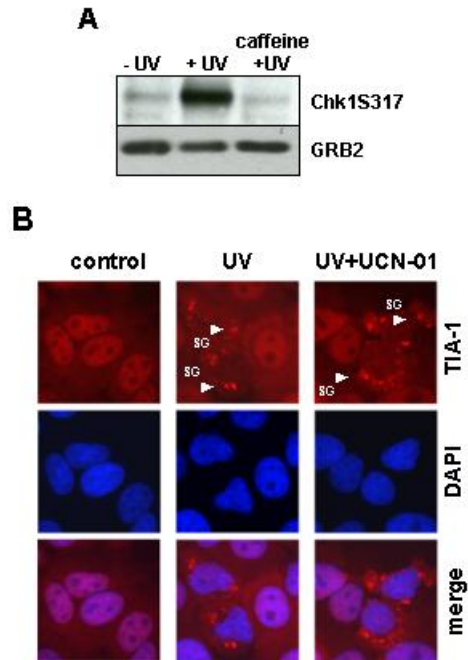


Figure S3. DDR kinases and SG formation.

A. Western blot analysis of ATR dependent CHK1 phosphorylation. Cells were UV irradiated (20 J/m^2) in the presence or absence of 8 mM caffeine and Chk1 phosphorylation was analyzed with an antiserum that specifically recognize phosphorylated Chk1.

B. TIA-1 staining of SGs after treatment with Chk1 and MK2 kinase inhibitor UCN-01 and 20 J/m^2 UV irradiation. HeLa cells were treated with UCN-01 for 2 h prior being subjected to 20 J/m^2 UV irradiation Cells have been processed 4h after UV exposure and analyzed by indirect immunofluorescence with an antibody that specifically recognized TIA-1.

Figure S4

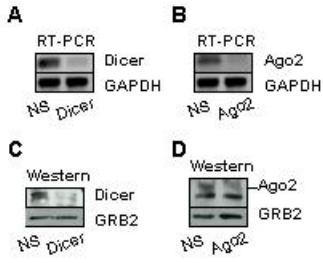


Figure S4. RT-PCR and Western blot analysis of Ago2 and Dicer expression after treatment of HeLa cells with 50 nM Ago2 or Dicer siRNAs for 72 hours.

Figure S5

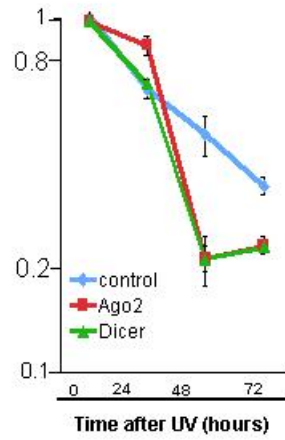


Figure S5. Cell proliferation after Ago2 and Dicer depletion.

The relative number of viable cells treated with a control, Ago2 or Dicer siRNA was measured at 0, 24, 48 and 72 hours after plating.

Table S1. Primers used for RT-PCR and gene knockdown experiments.

RT-PCR primers

Dicer

Pr1 5'-CAT-GGA-TAG-TGG-GAT-GTC-AC-3'

Pr2 5'-CTA-CTT-CCA-CAG-TGA-CTC-TG-3'

Ago2

Pr1 5'-CGC-GTC-CGA-AGG-CTG-CTC-TA-3'

Pr2 5'-TGG-CTG-TGC-CTT-GTA-AAA-CGC-T-3'

GAPDH

Pr1 5'-ACC-ACA-GTC-CAT-GCC-ATC-AC-3'

Pr2 5'-TCC-ACC-ACC-CTG-TTG-CTG-TA-3'

siRNA primers

Dicer duplex

Pr1 5'-CAT-GGA-TAG-TGG-GAT-GTC-AC-3'

Pr2 5'-CTA-CTT-CCA-CAG-TGA-CTC-TG-3'

Ago2 duplex

Pr1 5'-GCA-CGG-AAG-UCC-AUC-UGA-AUU-3'

Pr2 5'- pUUC-AGA-UGG-ACU-UCC-GUG-CUU-3

Non-specific duplex

Pr1 5'-AAU-UUU-UUU-CCC-CAA-AGG-GGG-3

Pr2 5'-AAC-CCC-CUU-UGG-GGA-AAA-AAA-3'
